UNCLASSIFIED

AAEC/E 121

AAEC/E 121

AUSTRALIAN ATOMIC ENERGY COMMISSION
RESEARCH ESTABLISHMENT
LUCAS HEIGHTS

SINTERING BY VOLUME DIFFUSION

by

M. J. BANNISTER

Issued Sydney, June 1964

UNCLASSIFIED

AUSTRALIAN ATOMIC ENERGY COMMISSION
RESEARCH ESTABLISHMENT
LUCAS HEIGHTS

SINTERING BY VOLUME DIFFUSION

by

M. J. BANNISTER

ABSTRACT

The process of sintering by volume diffusion has been subjected to a critical review. Various stages in the sintering process have been identified. It has been shown that sintering is most effective when the porosity takes the form of continuous pore channels along three-grain edges. The conditions determining when this stage finishes have been derived, and the effect of the subsequent stage on the sintering kinetics has been predicted. The available kinetic data for the sintering of BeO have been reviewed.

CONTENTS

1. INTRODUCTION

The term "sintering" is used in connection with the fabrication of many powdered materials, particularly ceramics such as beryllium oxide. It describes a process whose object may commonly be elimination of porosity, reduction of permeability, development of a suitable microstructure, or development of strength in a body. Sintering is a thermally activated process, and for refractory materials such as ceramics, short or prolonged heating at temperatures in the range 1000 – 2000 °C is generally involved. In this report, "sintering" is used synonymously with "densification", and refers to the elimination of porosity in a single phase, solid body.

To achieve an increase in density in a body during firing, material transport must occur. Mechanisms such as evaporation–condensation, volume diffusion, surface or grain–boundary diffusion, and viscous or plastic flow may all be responsible for the transport of material, although not all of these processes result in net densification (Postlethwaite and Shaler 1951). Experiments using alumina spheres (Kuczynski 1961), alumina powder compacts and ferric oxide powder compacts (Coble 1958), and BeO powder compacts (Aitken 1960) have indicated that in all these cases volume diffusion can best explain the behaviour observed during the initial sintering stage (up to 10 per cent. shrinkage). Since this stage is perhaps more amenable to exact theoretical treatment than any other it has been the subject of most reported studies. In practice most ceramists are interested in the later stages of the sintering process, that is from about 60 per cent. to 100 per cent. theoretical density. In this report the sintering phenomenon is analysed in this region of interest, with volume diffusion considered as the important mechanism of material transport.

2. REVIEW OF THE LITERATURE

2.1 Basic Assumptions

Most theories of sintering assume that pores or inter–particle neck surfaces act as vacancy sources (Kuczynski 1949; Coble 1961a) and that the excess vacancy concentration at such a source is given by the Kelvin equation:

$$\Delta C = \frac{C_0 \, \gamma \, a_0^3}{k \, T \rho} \quad . \tag{1}$$

(for the meanings of the symbols used in this and subsequent equations see Appendix I).

The flow of material during sintering is usually treated as a reverse flow of vacancies, and it has been shown (Kingery and Berg 1955; Burke 1957) that neighbouring grain boundaries are the most effective vacancy sinks. It is generally assumed (Coble 1961a) that the vacancy concentration at a representative grain boundary is equal to that found at a flat, free surface of the same material at the same temperature. The case of a material in which diffusion occurs by an interstitial rather than a vacancy mechanism may be treated by considering the pores to be sinks and the grain boundaries to be sources of interstitials.

Coble (1961a) has assumed that the length of the diffusion path between source and sink is of the same order of magnitude as the grain radius. This does not explain why pores appear to shrink rapidly only when they are adjacent to grain boundaries (Burke 1957). However, Hornstra (1961) has shown that when pores are located on moving, curved grain boundaries the average diffusion path length may be decreased by an order of magnitude. Thus for rapid sintering it is important to retain pores at grain boundaries during the sintering process.

2.2 Stages in the Sintering Process

According to Coble (1961a), there are three distinct stages in the sintering process:

Stage 1 – the growth of necks between particles.

Stage 2 – the shrinkage of pores present as continuous channels co–incident with three–grain edges in the material (henceforth called the cylindrical pore stage).

Stage 3 – the shrinkage of spherical pores located at four–grain corners.

Coble stated that an alternative final stage may involve spherical pores isolated within grains rather than at grain boundaries.

To facilitate his calculations, he assumed a grain structure of identical tetrakaidecahedra, and derived the following equation for Stages 2 and 3:

$$\frac{dP}{dt} = -\frac{A\,D_v\,\gamma\,a_o^3}{l^3\,kT} \quad , \qquad (2)$$

$$\text{where } A = \begin{cases} 10 & \text{for Stage 2} \\ \frac{6\pi}{\sqrt{2}} & \text{for Stage 3} \end{cases} \quad .$$

For alumina powder samples, with and without an additive of ¼ mole % MgO, it was found by Coble (1961b) and confirmed by Bruch (1962) that the grain growth kinetics during sintering followed the law:

$$l^3 - l_o^3 = Bt \quad . \qquad (3)$$

Coble combined Equations 2 and 3 to obtain the sintering equation:

$$P = H - J \log t \quad . \qquad (4)$$

He found (1961b) that cold pressed and sintered alumina compacts gave a linear relationship between porosity and log (time) from 60 to 95 per cent. of theoretical density and that the addition of ¼ mole % MgO both increased the rate of sintering and extended the linear relationship to about 98 per cent. of theoretical density. Bruch (1962) plotted his own data on a log – log basis, and found that for samples containing MgO, pressed and sintered under similar conditions to those used by Coble, an equation of the form:

$$P = K\,t^{-0.4} \qquad (5)$$

was obeyed to densities greater than 99 per cent. of theoretical. He showed that his and Coble's results agreed up to densities of about 94 per cent. of theoretical, but that at higher densities Coble's results indicated more rapid densification than Bruch had observed.

Coble found that the presence of ¼ mole % MgO prevented the isolation of pores within grains, which normally happened at about 98 per cent. of theoretical density. The addition of MgO thus permitted sintering to virtually theoretical density.

It is clear from the literature that other stages in the sintering process are also possible. Thus when suitable growth nuclei are present, the phenomenon known as "discontinuous" or "exaggerated" grain growth may occur. Suitable nuclei may be provided by large crystallites in the original powder (Cutler 1959), or by the unlocking of some, but not all, grain boundaries from the restraining pore phase (Burke 1957). The microstructure of a sample undergoing discontinuous growth shows a duplex grain structure, with large grains growing at the expense of their much smaller neighbours. Under these conditions the rate of growth of the large grains obeys the equation:

$$G - G_o = b\,t \qquad (6)$$

(Cutler 1959). The effect of discontinuous growth on the sintering kinetics is discussed in Section 5 of this report.

In the alternative final stage of sintering described by Coble, there are two possibilities. These depend on the relationship between the driving force for grain growth, and the restraining force exerted by the randomly distributed, spherical pores on the grain boundaries. It has been shown (McLean 1957) that these forces are approximately equal when

$$P = \frac{4}{3}\,\frac{r}{R} \quad . \qquad (7)$$

If the restraining force is less than the driving force, then for a pure material the rate of grain growth should obey the normal kinetic law:

$$G^2 - G_o^2 = f\,t \tag{8}$$

(Daniels et al. 1962). Under these conditions only a small fraction ($\sim 6r/R$) of the pores is in contact with grain boundaries at any given time, and thus the rate of densification should be quite low. If, however, the restraining force is equal to the driving force, then further grain growth becomes dependent on pore movement and/or shrinkage. Under these conditions the pores are "swept up" by the moving gfain boundaries (see Burke 1957). It would be expected that during this stage the residual porosity would be related to the total number of grains present.

2.3 Sintering and Grain Growth Data for BeO

There is a dearth of good experimental data on the kinetics of sintering and grain growth in BeO. Most investigators have varied only the sintering temperature, without studying the rate of sintering at any particular temperature.

Aitken (1960) studied the initial shrinkage kinetics of BeO pellets in the range 1160 – 1385 °C using a dilatometric technique. His results apparently fitted the predictions of a volume diffusion model, with an activation energy of about 150 kcal/mole. In the presence of ¼ mole % MgO, shrinkage was more rapid and the activation energy was reduced to about 100 kcal/mole. By contrast, Quirk (1959) found an activation energy of about 249 kcal/mole for the initial shrinkage of an impure grade of BeO over the same temperature range.

Felten (1961) studied the sintering and grain growth kinetics of an oxalate-derived BeO at one temperature only; 1700 °C. He fitted his sintering results to a log-linear plot of the type used by Coble (1961b) for alumina, and found that the grain size was directly proportional to time up to a density of about 95% theoretical. Subsequent grain growth obeyed a cube law of the type observed by Coble during the sintering of alumina. While Felten concluded that the linear grain growth period was indicative of discontinuous growth, the microstructures presented showed no evidence of the duplex grain structure which would be expected if discontinuous growth had occurred.

3. THE FORCES BETWEEN PORES AND GRAIN BOUNDARIES

Burke (1957) has suggested that pores may act as inclusions to prevent or restrict grain growth. The simple theory generally proposed (McLean 1957) takes as its model a random dispersion of identical spherical inclusions. Under optimum sintering conditions, however, one is interested in the effect of porosity that is totally coincident with grain boundaries. Using simple models based on the one used by McLean (1957), the author has made calculations for cylindrical pores at three-grain edges and grain boundaries, and for spherical pores at four-grain corners, three-grain edges, and grain boundaries. The results of these calculations are given in Table 1.

However, Walker (A.A.E.C. private communication) has pointed out that the simple model as given by McLean (1957) under-estimates the values of the forces involved. True forces should be calculated from a work-energy consideration. For the simplest case of a spherical pore at a grain boundary, the true maximum force resisting displacement of the pore to the grain interior is then $2\pi\lambda r$, or twice the value given by the McLean treatment. For a cylindrical pore at a three-grain edge (Figure 1) the work-energy calculation gives the value of the resolved force F_x between the pore and the grain boundaries as:

$$F_x = \lambda l \left[\frac{x \sin^2 \alpha}{\sqrt{r^2 - x^2 \sin^2 \alpha}} + \frac{x \sin^2 \beta}{\sqrt{r^2 - x^2 \sin^2 \beta}} + \frac{x \sin^2 \theta}{\sqrt{r^2 - x^2 \sin^2 \theta}} + \cos \alpha + \cos \beta - \cos \theta \right] \tag{9}$$

For any values of the angles α, β, and θ, F_x has its greatest value when x is a maximum, that is when $x = r$. Equation 9 then becomes:

$$F_x = \lambda l \left[\frac{1}{\cos \alpha} + \frac{1}{\cos \beta} + \frac{\sin^2\theta - \cos^2\theta}{\cos\theta} \right] \quad . \tag{10}$$

In the case where the migrating three–grain edge tends to leave the cylindrical pore behind at a grain boundary, we can put

$$\theta = 0 \ , \ \alpha = \beta \ .$$

Thus

$$F_x = \lambda l \left[\frac{2}{\cos \alpha} - 1 \right] \quad . \tag{11}$$

In the absence of the pore the equilibrium value of α would be 60°, and substitution in Equation 11 gives:

$$F_x\ (\alpha = 60°) = 3\,\lambda l \ .$$

However in the presence of the pore a lower value of α might be expected, owing to the drag exerted by the pore on the three–grain edge. For the lowest possible value, $\alpha = 0$, Equation 11 gives:

$$F_x\ (\alpha = 0°) = \lambda l \ .$$

F_x would thus be expected to have a value between λl and $3\,\lambda l$, the exact value depending on possible distortion of the migrating grain boundaries. The McLean treatment gives $F_x = \lambda l$ (Table 1).

The other conditions listed in Table 1 could also be treated by the work–energy method. The most interesting case is that of spherical pores situated at four–grain corners, the configuration proposed by Coble (1961a) as Stage 3 in the sintering process. The necessary calculations are very complex and will not be given here. The calculated value of the maximum force exerted by a spherical pore on a migrating four–grain corner is $1.35\ \lambda r$, whereas the McLean treatment gives $0.75\ \lambda r$ (Table 1).

These results enable us to predict the effectiveness of pores in restraining grain growth. Thus, assuming a tetrakaidecahedral grain shape with all the porosity contained at grain surfaces:

$$\text{Volume of pores per unit grain boundary area} = \frac{P\,l}{1.2} \quad . \tag{12}$$

For the cylindrical pore stage, the minimum force required to displace a pore from a three–grain edge is <u>at least</u> λl. Thus the maximum force per unit area exerted by the pores on the grain boundary is at least:

$$F_R = \frac{P\,l}{1.2} \cdot \frac{1}{\pi a^2 l} \cdot \lambda l \quad . \tag{13}$$

The driving force per unit area for grain growth is (McLean 1957):

$$F_D = \frac{2\lambda}{R} \ , \tag{14}$$

where R is the effective grain radius. Unlocking of cylindrical pores from three–grain edges will <u>not</u> occur if:

$$F_D < F_R \quad . \tag{15}$$

Now $\quad P = 1.06\,\pi\,\frac{a^2}{l^2}$ (Coble 1961a).

(Note that Coble omitted the factor π).

Substitution in Equation 15 yields:

$$2.3\,l < R \tag{16}$$

as the condition for cylindrical pores to remain at three–grain edges.

For the tetrakaidecahedral grain model used, R is of course infinite and thus Equation 16 is always fulfilled. Alternatively if we assume that R is the radius of the sphere having the same volume, or surface area, as the model grain, then $R = 1.39\, l$, or $R = 1.46\, l$, respectively. In an average compact during sintering, the value of R would be between $1.39\, l$ and infinity, and should generally be greater than $2.3\, l$. Thus from Equation 16 we would expect that cylindrical pores would remain at three-grain edges during the cylindrical pore stage of sintering.

By similar reasoning to that used above, and taking the value $1.35\, \lambda r$ for the force exerted on a migrating grain boundary by a spherical pore at a four-grain corner, we find that spherical pores will remain trapped at four-grain corners only if:

$$3.35\, l^2 < r R \quad . \tag{17}$$

In general, pore spheroidization is found to occur below about 5 per cent. porosity (Coble 1961b), at which Coble's equation $P = \frac{\pi}{\sqrt{2}} \frac{r^3}{l^3}$ for spherical pores at four-grain corners, gives $r/l = 0.28$. Substitution in Equation 17 gives:

$$12\, l < R \tag{18}$$

as the condition which must be fulfilled if spherical pores at a porosity of 5 per cent. are to be maintained at four-grain corners. Such a condition is unlikely to be met by more than a few grains during sintering. Thus Coble's stage 3 in the sintering process would not be expected to occur unless some additional boundary-locking agents besides pores were present in the structure. The spheroidization of cylindrical pores should herald the isolation of pores from grain boundaries.

4. THE SPHEROIDIZATION OF CYLINDRICAL PORES

The driving force for spheroidization is provided by the tendency towards the reduction of total free energy for the system. Three approaches to the problem are used in this section. These involve calculations to determine when spheroidization is energetically possible, when it is geometrically likely, and when the rate of spheroidization is likely to become significant.

4.1 The Energetics of Pore Spheroidization

The model used is one in which a network of cylindrical pores along three-grain edges gives a spherical pore at each four-grain corner after spheroidization. In the neighbourhood of any four-grain corner, four cylindrical pores each 1/2 units long give one spherical pore at the corner. The increase in energy per four-grain corner associated with this change is:

$$\Delta E = (4\pi r^2 \gamma - 5.7 r^2 \lambda) - (4\pi a l \gamma - 6 a l \lambda) \quad . \tag{19}$$

If pore volume is conserved, we have:

$$2\pi a^2 l = \frac{4}{3} \pi r^3 \quad . \tag{20}$$

Also $\quad P = 1.06\pi \frac{r^2}{l^2}$ (Coble 1961a) .

Spheroidization is energetically favourable when:

$$\Delta E \leqslant 0 \quad , \tag{21}$$

These equations have been used to calculate values of the porosity at which spheroidization may begin, for various values of γ/λ. The results are given in Table 2.

For metals, the value of γ/λ is generally somewhere near 3 (McLean 1957). It is apparent that pore spheroidization is energetically possible very early in the sintering process.

4.2 Steric Requirements of Pore Spheroidization

An obvious requirement of pore spheroidization is that the spherical pores formed should not overlap. Thus $r \leqslant l/2$. Using the equation

$$P = \frac{\pi}{\sqrt{2}} \frac{r^3}{l^3} \quad ,$$

we find that:

$$P \leqslant 0.278 \ .$$

A more restrictive requirement may be obtained by considering the state of affairs when the centre of a cylindrical pore is just about to be pinched off. An axial section of a model pore is shown in Figure 2. The earliest stage at which the pore channel closes occurs when $a = l/2$. In this case the volume of each half-pore is $a^3 \pi \left(\frac{5}{3} - \frac{\pi}{2}\right)$. Four of these combine to form each spherical pore after spheroidization. Since the cylindrical pores overlap one another at four-grain corners, some reduction in the net volume per half-pore is necessary. This correction is difficult to calculate, but a volume reduction of half does not seem unreasonable. This would give a residual porosity of 0.041 (4.1 per cent.) when pores begin to close. If no correction for overlap is made, the corresponding calculated porosity is 0.083 . The value of about 4 per cent. is in good agreement with the porosity at which pore closure is often observed to begin (Coble 1961b).

4.3 The Rate of Pore Spheroidization

Even when a cylindrical pore channel closes off, the residual porosity is not immediately converted to spherical pores. Also we would expect that so long as the porosity extends along the greater part of any three-grain edge, pores will remain at grain boundaries. A very simplified model which describes the spheroidization of a closed-end, cylindrical pore is shown in Figure 3. We take the criterion for effective pore spheroidization to be:

$$-\frac{dx}{dT} < -\frac{1}{a}\frac{dy}{dT} \ . \tag{22}$$

Now

$$-\frac{dy}{dT} = V_1 - V_2 - V_3 \frac{\delta}{l} \ , \tag{23}$$

and

$$-\frac{dx}{dT} = V_4 + V_3 \frac{\delta}{a} \ . \tag{24}$$

Also

$$V_1 = \frac{4 D_V a_o^3 \gamma}{kTa\,l} \quad \text{(Coble 1961a)} \ ,$$

$$V_2 = \frac{D_V a_o^3 \gamma}{2k\,Ta\,l}$$

(on the assumption that about one quarter of the flux V_4 deposits along the cylindrical pore wall) ,

$$V_3 = \frac{2 D_S \gamma a_o^3}{k\,Ta^2}$$

(by analogy with Kuczynski 1949 and Coble 1961a) ,

and

$$V_4 = \frac{2 D_V a_o^3 \gamma}{k\,Ta^2} \quad \text{(Coble 1961a)} \ .$$

Combination of all these equations yields:

$$\frac{D_S}{D_V} > \frac{3a}{8\delta} \tag{25}$$

or, to prevent effective spheroidization:

$$\frac{D_s}{D_v} < \frac{3a}{8\delta} \quad . \qquad (26)$$

This result is only qualitative, of course, but it does indicate that the value of the ratio D_s/D_v has a strong influence on the pore size at which the rate of spheroidization becomes effective. It is suggested that the effect of MgO in aiding the sintering of alumina to high densities (Coble 1961b) might be due to its influence on the ratio D_s/D_v. An increase in the value of D_v without a proportional increase in D_s would explain the observed effects of MgO on the densification of alumina, which include an increase in densification rate (see Equation 2) as well as the attainment of higher densities.

5. GRAIN GROWTH DURING THE CYLINDRICAL PORE STAGE

The following results were obtained during the sintering of alumina:

(a) The grain growth equation was:

$$G^3 - G_o^3 = cT \qquad (27)$$

(Coble 1961b, Bruch 1962); this equation was purely experimental.

(b) The activation energy for grain growth was equal to the activation energy for densification, and its magnitude (~ 150 kcal/mole) indicated that a volume diffusion mechanism was the rate-determining factor (Coble 1961b, Bruch 1962).

(c) The presence of 1/4 mole % mgO had no effect on the rate of grain growth, so long as the pores had not spheroidized (Coble 1961b).

(d) The rate of grain growth was independent of the green density of the samples (Bruch 1962).

(e) At low temperatures and low green densities, the sintering rate became abnormally low. This effect could be overcome by using higher green densities and/or higher sintering temperatures (Bruch 1962). The pores increased in size (but decreased in number) under these "subnormal" sintering conditions.

For pores to be maintained at grain boundaries, despite grain growth, during the cylindrical pore stage (see Section 2), then either:

(i) pores move with grain boundaries,

or (ii) the boundaries only move as they are released by pore closure.

Alternative (ii) seems to be discounted by (d) above.

If pores move with grain boundaries, then either:

(iii) the rate of grain growth is dependent on the rate of pore movement,

or (iv) the rate of grain growth depends on some process that is slower than the possible rate of pore movement.

The effect of temperature on the phenomenon mentioned in (e) indicates that a modification in pore structure may occur by some process (for example surface diffusion) with a lower activation energy than that needed for densification. Hey and Livey (1962) found that a detrimental change in pore structure, without any densification, occurred when an impure grade of BeO was heated to moderate temperatures. Thus it does seem possible that in some cases at least pores could move readily by a surface diffusion mechanism.

In normal, unimpeded grain growth, the grain boundary movement can be considered as resulting from the flow of vacancies across a grain boundary of constant width ϵ, and between a vacancy concentration difference proportional to $1/G$. Integration of the diffusion equation gives the equation for grain growth under these conditions (Equation 8). If the presence of cylindrical pores modifies the vacancy diffusion path so that its length becomes proportional to the grain size G, then integration of the diffusion equation would give an equation for grain growth of the form of Equation 27. Such a diffusion path would probably imply a volume diffusion mechanism (see observation (b)) and might fit in with the observed independence of grain growth rate on the green density (observation (d)). However it is not clear how the presence of cylindrical pores could affect the vacancy diffusion path in this way.

6. SINTERING DURING DISCONTINUOUS GRAIN GROWTH

The reasons for discontinuous grain growth have been discussed in Section 1. During this stage, pores are located within the large growing grains and at the boundaries of the smaller grains. Since only those pores at grain boundaries are able to shrink, an impingement factor must be introduced into the densification equation that would have prevailed in the absence of discontinuous growth. This factor is $(1-v)$ where v is the volume fraction of large growing grains present, or $[1-(t/t_i)^3]$ where t is the time interval from the start of discontinuous growth, and t_i is the time needed for the completion of discontinuous growth. Thus the substitution of the impingement factor in Equation 4 yields:

$$P(1-v) = H - J \log t \quad . \qquad (28)$$

It can be seen that the effect of the impingement factor becomes noticeable only during the last half of the period during which discontinuous growth occurs.

7. SUMMARY

Various stages in the process of sintering by volume diffusion have been identified. They may be summarised as follows:

(a) Neck formation

This period may cover the first ten per cent. of the total possible shrinkage.

(b) The cylindrical pore stage

During this period, which may extend to greater than 96 per cent. of theoretical density, the porosity-time relationship may obey an equation of the form:

$$P = H - J \log t \quad . \qquad (4)$$

For alumina, the rate of grain growth during this stage has been observed to follow an equation of the form:

$$G^3 = G_o^3 + ct \quad . \qquad (27)$$

(c) The discontinuous grain growth stage

For powders of reasonably uniform initial particle size, discontinuous grain growth would follow the cylindrical pore stage. The densification equation may take the form:

$$P[1-(t/t_i)^3] = H - J \log t \quad . \qquad (28)$$

The rate of growth of the discontinuously growing grains obeys the equation:

$$G - G_o = bt \quad . \qquad (6)$$

(d) Unimpeded or normal grain growth stage

This would follow the impingement of discontinuously growing grains. The rate of densification would be slow during this period, and the rate of grain growth should follow the equation:

$$G^2 - G_o^2 = ft \quad . \tag{8}$$

(e) Restricted grain growth stage

This condition occurs when the grains are so large that their further movement becomes dependent on pore shrinkage or pore movement. Equations for the rates of grain growth and densification during this stage have not been proposed. Note that although (a) to (e) should follow one another in order, the later stages may not always be observed.

The occurrence of Coble's Stage 3, involving shrinkage of spherical pores at four-grain corners, has been shown to be unlikely. The importance of the cylindrical pore stage has been demonstrated, and the conditions governing the ending of this stage have been determined. The topic of grain growth in the presence of cylindrical pores has been discussed, with reference to the published work on alumina.

From a review of the available sintering data for BeO it is apparent that further experimental work, particularly in the range 60 – 100 per cent. of theoretical density, must be performed before the sintering behaviour of BeO can be understood.

8. ACKNOWLEDGMENTS

The author is grateful to Dr. K. D. Reeve and Dr. D. G. Walker for their helpful criticism of this work.

9. REFERENCES

Aitken, E.A. (1960). – J. Amer. Ceram. Soc. 43: 627.

Bruch, C.A. (1962). – Bull. Amer. Ceram. Soc. 41: 799.

Burke, J.E. (1957). – J. Amer. Ceram. Soc. 40: 80.

Coble, R.L. (1958). – J. Amer. Ceram. Soc. 41: 55.

Coble, R.L. (1961a). – J. Appl. Physics 32: 787.

Coble, R.L. (1961b). – J. Appl. Physics 32: 793.

Cutler, I.B. (1959). – Kinetics of High Temperature Processes. (Ed. W. D. Kingery) Technology Press of M.I.T., and Wiley, N.Y.

Daniels, A.V. Jr., Lowrie, R.C. Jr., Gibby, R.L., and Cutler, I.B. (1962). – J. Amer. Ceram. Soc. 45: 282.

Felten, E.J. (1961). – J. Amer. Ceram. Soc. 44: 251.

Hey, A.W., and Livey, D.T. (1962). – AERE-R3870.

Hornstra, J. (1961). – Physica 27: 342.

Kingery, W.D., and Berg, M. (1955). – J. Appl. Physics 26: 1205.

Kuczynski, G.C. (1949). – J. Metals 1: 169.

Kuczynski, G.C. (1961). – Powder Metallurgy. (Ed. W. Leszynski) Interscience, N.Y.

McLean, D. (1957). – Grain Boundaries in Metals. Clarendon Press, Oxford.

Postlethwaite, A.W., and Shaler, A.J. (1951). – The Physics of Powder Metallurgy. (Ed. W. E. Kingston) McGraw-Hill, N.Y.

Quirk, J.F. (1959). – J. Amer. Ceram. Soc. 42 : 178.

APPENDIX 1

DEFINITIONS OF SYMBOLS USED

a	Radius of a cylindrical pore
a_o^3	Volume of a lattice vacancy
b	A constant for a given material at a given temperature
c	A constant for a given material at a given temperature
f	A constant for a given material at a given temperature
k	The Boltzmann constant
l	Length of a cylindrical pore, or a tetrakaidecahedron edge
r	Radius of a spherical pore
t	Time
t_i	The time required for the completion of discontinuous growth
v	The volume fraction of discontinuously-growing grains
x	A co-ordinate direction
y	A co-ordinate direction
A	A geometrical constant
B	A constant for a given material at a given temperature
C_o	The equilibrium concentration of vacancies under a free, flat surface
ΔC	The difference in vacancy concentration
D_v	The coefficient of volume diffusion for the rate-determining ionic species
D_s	The coefficient of surface diffusion for the relevant ionic species
ΔE	The energy increase after spheroidization
F_x	The force in the x direction
F_D	The driving force per unit area of grain boundary
F_R	The restraining force per unit area of grain boundary
G	Grain size
H	A constant
J	A constant for a given material at a given temperature
K	A constant for a given material at a given temperature

APPENDIX 1 (continued)

P	The total porosity
R	The effective grain radius
T	The absolute temperature
V_1	The vacancy volume per unit time diffusing from unit area of cylinder wall to grain boundaries
V_2	The vacancy volume per unit time diffusing to unit area of cylinder wall from hemispherical end
V_3	The vacancy volume per unit time diffusing from hemispherical end, through unit area of cylinder/hemisphere boundary to cylinder wall
V_4	The vacancy volume per unit time diffusing from unit area of hemisphere to grain boundaries and to the cylinder walls
γ	Surface energy
δ	The effective depth over which surface diffusion occurs
ϵ	The width of a grain boundary
λ	Grain boundary energy
θ	An angle
ρ	Radius of curvature of a surface
α	An angle
β	An angle

TABLE 1

THE FORCES BETWEEN PORES AND GRAIN BOUNDARIES   McLEAN MODEL

Pore	Where Situated	Displaced To	Force
Cylindrical, length l	Grain boundary	Grain interior	$2\lambda l$
,, ,, ,,	3–grain edge	Grain boundary	λl
,, ,, ,,	,, ,, ,,	Grain interior	$3\lambda l$
Spherical, radius r	Grain boundary	Grain interior	$\pi\lambda r$
,, ,, ,,	3–grain edge	Grain boundary	$2\lambda r$
,, ,, ,,	,, ,, ,,	Grain interior	$6\lambda r$
,, ,, ,,	4–grain corner	3–grain edge	$\frac{3}{4}\lambda r$
,, ,, ,,	,, ,, ,,	Grain interior	$4.9\lambda r$

TABLE 2

THE SPHEROIDIZATION OF CYLINDRICAL PORES

γ/λ	Spheroidization Possible for P less than
1	0.511
3	0.628
10	0.651

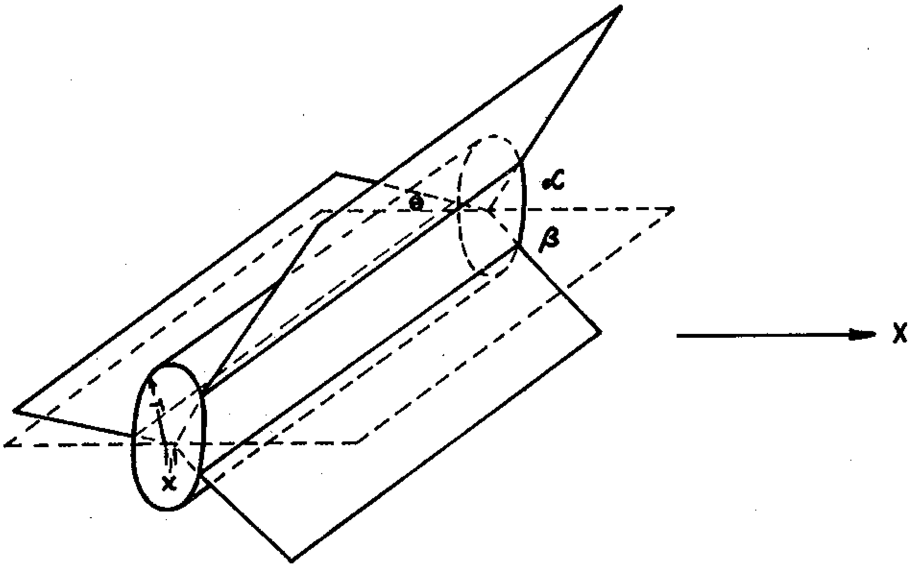

Figure 1. A CYLINDRICAL PORE AT A THREE – GRAIN EDGE

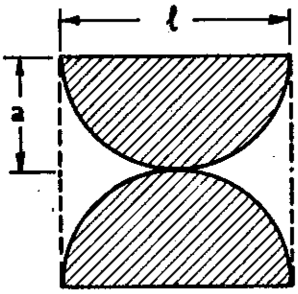

Figure 2. A CYLINDRICAL PORE THAT HAS JUST CLOSED

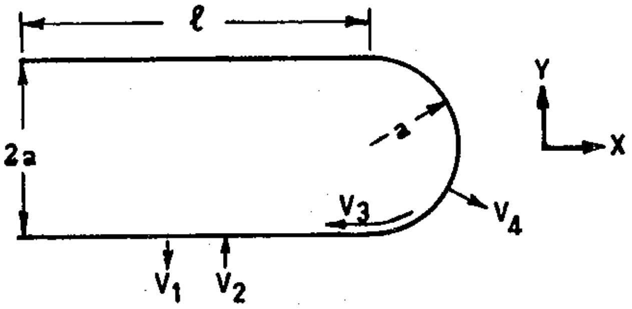

Figure 3. A CLOSED - END CYLINDRICAL PORE

P617